Neotropical Ichthyology

Original article

https://doi.org/10.1590/1982-0224-2025-0209

urn:lsid:zoobank.org:pub:2528A7FF-F76F-4242-87A1-29BB9C414ACC

A new species of *Tridensimilis* (Siluriformes: Trichomycteridae) from Tapajós basin: the largest translucent catfish species of Tridentinae

Correspondence:
André L. Colares Canto
cantoandre@gmail.com

André L. Colares Canto[1], Aléssio Datovo[2], Willian M. Ohara[3], Mário C. C. de Pinna[2] and Frank Raynner V. Ribeiro[1]

A new species of translucent catfish of the genus *Tridensimilis* is described from the upper and middle rio Tapajós basin, states of Pará and Mato Grosso, Brazil. In addition, we redefine the taxonomic limits of the genus *Tridensimilis* and present evidence that questions the current generic placement of *Tridentopsis tocantinsi*. The new species is distinguished from congeners by a set of morphological features, in combination: number of vertebrae, anal-fin rays, opercular and interopercular odontodes; eyes positioned laterally and oriented ventrally, slightly more visible in ventral than in dorsal view; and basipterygia fused at midline. Live specimens of the new species display *ex situ* atmospheric air capture at the water surface, resulting in the filling of the digestive cavity with air bubbles, a behavior recorded for the first time in any representative of Tridentinae. The new species is the largest currently known of the subfamily Tridentinae, with analyzed specimen reaching 34 mm of standard length. The new taxon likely increases the list of endemism in the rio Tapajós basin.

Keywords: Amazon basin, Behavior, Biodiversity, Conservation, Taxonomy.

Submitted December 6, 2025
Accepted March 13, 2026
Epub ???, 2026

Associate Editor Carlos DoNascimiento
Section Editor Bruno Melo
Editor-in-chief José Birindelli

1 Instituto de Ciências e Tecnologia das Águas, Universidade Federal do Oeste do Pará, Rua Vera Paz, s/n, 68040-255, Santarém, PA, Brazil. (ALCC) cantoandre@gmail.com (corresponding author), (FRVR) fraynner@yahoo.com.br.

2 Museu de Zoologia da Universidade de São Paulo (MZUSP), Av. Nazaré, 481, Ipiranga, 04263-000, São Paulo, SP, Brazil. (AD) adatovo@usp.br, (MCCP) pinna@ib.usp.br.

3 Universidade Federal do Amazonas, Departamento de Biologia, Av. Rodrigo Otávio Japiim, 69077-000, Manaus, AM, Brazil. (WMO) ohara@ufam.edu.br.

Online version ISSN 1982-0224
Print version ISSN 1679-6225

Neotrop. Ichthyol.
vol. 24, no. 2, 2026

Uma nova espécie de bagre translúcido do gênero *Tridensimilis* é descrita do rio Teles Pires e trechos alto e médio do rio Tapajós, nos estados do Pará e Mato Grosso, Brasil. Além disso, redefinimos os limites taxonômicos do gênero *Tridensimilis* e apresentamos evidências que questionam a atual classificação genérica de *Tridentopsis tocantinsi*. A nova espécie distingue-se de suas congêneres por um conjunto de características morfológicas em combinação: número de vértebras, raios da nadadeira anal e odontódios operculares e interoperculares; olhos posicionados lateralmente e orientados ventralmente, ligeiramente mais visíveis em vista ventral do que em vista dorsal; e basipterígios fusionados na linha mediana. Exemplares vivos da nova espécie exibem a captura de ar atmosférico *ex situ* na superfície da água, resultando no preenchimento da cavidade digestória com bolhas de ar, um comportamento registrado pela primeira vez para representante de Tridentinae. A nova espécie é a maior atualmente conhecida para a subfamília Tridentinae, com exemplar analisado atingindo 34 mm de comprimento padrão. O novo táxon provavelmente aumenta a lista de endemismos na bacia do rio Tapajós.

Palavras-chave: Bacia Amazônica, Biodiversidade, Comportamento, Conservação, Taxonomia.

INTRODUCTION

Tridentinae is a subfamily of Neotropical translucent catfish established by Eigenmann (1918). Its taxonomic history began with the proposition of the genus *Tridens* Eigenmann & Eigenmann, 1889 to allocate two new species, *T. melanops* Eigenmann & Eigenmann, 1889, and *T. brevis* Eigenmann & Eigenmann, 1889 (= *Tridentopsis brevis*). Currently, Tridentinae is recognized as a monophyletic group composed of five genera and eleven valid species (Baskin, 1973; de Pinna, 1998; DoNascimiento, 2013; Ochoa *et al*., 2017, 2020; Datovo *et al*., 2023; Henschel *et al*., 2023) and is the least diverse subfamily within the TSVSGM group (Fricke *et al*., 2025a). Tridentines are widely distributed throughout South America, in the basins of the Amazon, Tocantins, Maracaibo, Orinoco, and Paraguay rivers (Fricke *et al*., 2025a).

The taxonomic knowledge of Tridentinae species remains limited. Most of its species are known exclusively from their original descriptions published over a century ago, primarily based on external morphological traits and a limited set of osteological characters (Datovo *et al*., 2023; Henschel *et al*., 2023). The scarcity of taxonomic information is exemplified by *Tridentopsis brevis* (Eigenmann & Eigenmann, 1889), described based on the unique holotype, now missing for over a century and probably lost (Schultz, 1944). Recent taxonomic efforts, such as the description of two new species of *Tridens* (*T. vitreus* Henschel, Ohara & Costa, 2023 and *T. chicomendesi* Henschel & Costa, 2023) and of the genus *Rhinotridens* Datovo, Ochoa, Vita, Presti, Ohara & Pinna, 2023 (*R. chromocaudatus* Datovo, Ochoa, Vita, Presti, Ohara & Pinna, 2023 and *R. britskii* de Pinna, Reis, Pastana & Datovo, 2024), have improved our knowledge of the diversity of the group and reflect renewed taxonomic interest.

Baskin (1973) proposed a phylogenetic hypothesis for Tridentinae, providing five putative synapomorphies for a clade composed of *Tridens* and *Tridensimilis* Schultz, 1944: (1) fewer opercular teeth, (2) rictal barbel not visible externally, (3) eyes facing more ventrally than dorsally, (4) Weberian capsule with an elongate, neck-like lateral constriction, (5) anal-fin origin three or more vertebrae anterior to dorsal-fin origin. Datovo *et al.* (2023) described *Rhinotridens* and proposed the genus as sister group to the clade formed by *Tridens* plus *Tridensimilis* (Baskin, 1973), based on the shared presence of three to six opercular odontodes and a basipterygium that is mostly or entirely cartilaginous in adults. Datovo *et al*. (2023) also noted that one of the morphological characters used by Baskin (1973) for *Tridens* + *Tridensimilis* (rictal barbels not externally visible) is not corroborated as synapomorphic.

Tridensimilis is a monotypic genus of Tridentinae currently composed of *T. venezuelae* Schultz, 1944 only, from the Lake Maracaibo basin in Venezuela (Datovo *et al*., 2023). Here, we describe a second, distinctly diagnosable species of *Tridensimilis* found in the upper and middle stretches of the rio Tapajós basin. This discovery highlights the ongoing importance of scientific research in understanding and conserving the aquatic ecosystems of Amazonian river basins, which face increasing anthropogenic pressures.

MATERIAL AND METHODS

Measurements and counts were point-to-point, taken on the left side of specimens whenever possible, using a digital caliper with precision to nearest 0.01 mm, according to Tchernavin (1944) and Datovo *et al*. (2023). The measurement "ventral interorbital distance" is newly proposed to quantify the degree to which eyes are positioned more ventrally than dorsally (or vice-versa). Measurements are presented as percentages of standard length (SL) for subunits of the body or as percentages of head length (HL) for subunits of the head. Double-stained osteological preparations (c&s) followed Taylor, Van Dyke (1985). Anatomical nomenclature followed Arratia, Huaquin (1995) for the laterosensory system, de Pinna, Dagosta (2022) for soft-tissue structures of the head, and Datovo *et al*. (2023) for osteology. Osteological illustrations were made using a stereomicroscope equipped with a digital camera. Drawings were hand-rendered with a digital pen tablet from photographs and from direct observations of specimens under a stereomicroscope.

Counts of fin rays were taken from type specimens, absolute frequencies are given in parentheses throughout the description, and holotype counts are indicated with an asterisk. Counts of internal supports were obtained from c&s specimens. Fin-ray counts included unbranched rays (designated by Roman numerals) and all subsequent branched rays (denoted by Arabic numerals). Caudal-fin ray counts included all branched rays plus one unbranched ray in each lobe, with counts for upper and lower lobes separated by a plus sign. Vertebral counts included all post-Weberian vertebrae, with the compound caudal centrum (PU1+U1) counted as one. Institutional abbreviations follow Fricke, Eschmeyer (2025b).

RESULTS

Tridensimilis magnus, new species

urn:lsid:zoobank.org:act:6783B6B5-2631-4EBC-A539-9B7FAE9F5B8A

(Figs. 1–9; Tab. 1)

Holotype. MZUSP 131529, 30.6 mm SL, Brazil, Pará State, Itaituba Municipality, rio Tapajós basin, rio Jamanxim drainage, igarapé Branco, tributary to rio Aruri Grande, 05°24'9.07"S 55°52'59.01"W, 9 Oct 2019, A. Hercos.

Paratypes. All from Brazil, rio Tapajós basin. UFOPA-I 1773, 41, 6 c&s, 24.3–34.2 mm SL, collected with holotype. INPA-ICT 36887, 6, 23.6–26.5 mm SL, Pará State, Jacareacanga Municipality, igarapé Preto, tributary to rio Pacu, approx. 06°08'58.62"S 57°15'18.95"W, 7 Aug 2008, W. Pedroza. INPA-ICT 36888, 6, 1 c&s, 20.4–26.2 mm SL, Pará State, Jacareacanga Municipality, rio das Tropas, Babaçual, approx. 06°04'23.72"S 57°36'19.35"W, 27 Jul 2008, W. Pedroza. INPA-ICT 62041, 21, 20.3–25.2 mm SL, Pará State, Jacareacanga Municipality, rio Muiuçu, 06°18'35"S 57°59'43"W, 7 Jul 2023, W. Ohara & L. Tencatt. INPA-ICT 62042, 27, 17.3–25.7 mm

FIGURE 1 | *Tridensimilis magnus* in lateral, ventral, and dorsal views, holotype, MZUSP 131529, 30.6 mm SL, igarapé Branco, tributary to rio Aruri Grande, rio Jamanxim drainage, rio Tapajós drainage, Pará State, Brazil. Scale bar = 2.0 mm.

SL, Pará State, Jacareacanga Municipality, igarapé Limão, 06°03'07.5"S 57°48'38"W, 7 Jul 2023, W. Ohara & L. Tencatt. MZUSP 116486, 9, 18.1–28.2 mm SL, Mato Grosso State, Paranaita Municipality, rio São Benedito, tributary to rio Teles Pires, approx. 09°07'14.16"S 56°59'35.12"W, 4 Apr 2014, W. Ohara. UFOPA-I 1772, 1, 32.3 mm SL, Pará State, Trairão Municipality, rapids of Pimental, rio Tapajós, approx. 04°34'07.5"S 56°15'51.1"W, 24 Nov 2021, A. Conceição, J. Sarino, A. Dias, D. Salomão & M. Lima. UFOPA-I 1774, 8, 2 c&s, 20.4–24.7 mm SL, Pará State, Jacareacanga Municipality, igarapé do Limão, 06°05'18.98"S 57°48'38"W, 7 Jul 2023, W. Ohara & L. Tencatt.

Diagnosis. *Tridensimilis magnus* differs from all other Tridentinae in having the largest body length, reaching 34 mm SL (*vs.* 27 mm in *Tridens*, 25 mm in *Tridentopsis* Myers, 1925, 17 mm in *Miuroglanis* Eigenmann & Eigenmann, 1889, 18 mm in *Rhinotridens*, and 23 mm in *Tridensimilis*). The new species is further distinguished from all tridentines, except *Rhinotridens britskii*, by having 39–41 post-Weberian vertebrae (*vs*. 34–38 in *Miuroglanis*, *Rhinotridens chromocaudatus*, *Tridentopsis* and *Tridensimilis*, and 45–52 in *Tridens*). *Tridensimilis magnus* additionally differs from *Tridensimilis venezuelae* and *T. tocantinsi* LaMonte, 1939, in having longer maxillary barbels that surpass the opercular odontophore (*vs.* not extending beyond pupil); externally visible rictal barbels reaching the base of interopercular odontophores (*vs*. rictal barbels not externally visible or reaching at most one-third of distance from their base to anterior margin of eyes); 7 or 8 dorsal-fin rays (*vs.* 8–11); and pelvic-fin base vertically aligned with the 13th or 14th vertebra (*vs.* with the 11th vertebra). The new species is additionally distinguished from *T. tocantinsi* in having 6 or 7 opercular odontodes (*vs.* 10); from *T. venezuelae* by having 7 or 8 interopercular odontodes (*vs.* 4–6).

Description. Morphometric data in Tab. 1. Body elongated, greatest body depth at vertical through urogenital and anal openings. Dorsal profile of trunk mostly straight, gradually expanding from snout tip to dorsal-fin base. Ventral trunk profile nearly straight from snout tip to end of pectoral fin, then convex to anal-fin base. Caudal peduncle strongly compressed. Dorsal and ventral profile of caudal peduncle gradually expanding with procurrent rays. Axillary gland present, originating around base of pectoral fin and extending posteriorly to approximately half of fin length.

Head depressed, forming a curvilinear triangle shape in dorsal view. Eyes round, large, approximately 25% of head length, positioned laterally on midlength of head; more exposed ventrally than dorsally, lacking free orbital margin; covered by thin and translucent integument. Anterior nostril surrounded by membrane forming short tube extending a lateral flap; posterior nostril near anterior margin of eye, with integument rim forming a short flap. Mouth ventral, slightly curved at rictus in ventral view; upper lip with integument folds continuous with rictal barbel base.

Opercular and interopercular odontodophores juxtaposed, located on posterior third of head. Interopercular odontodophore slightly shorter and deeper than opercular one, round posteriorly, lateroventrally positioned on head, and slightly anterior to opercular one, with 7 or 8 conical odontodes. Opercular odontodophore distally round, shorter and narrower than interopercular one, dorsolaterally positioned on head, reaching dorsal margin of pectoral-fin base, with 6 or 7 conical odontodes. Branchial membrane narrowly attached to isthmus at midline.

TABLE 1 | Morphometric data of holotype and 19 paratypes of *Tridensimilis magnus*. Range includes the holotype. SD = Standard deviation.

	Holotype	Range	Mean	SD
Standard length (mm)	30.6	19.9–33.9		
Percentage of standard length				
Body depth	16.3	13.1–16.3	14.9	0.9
Caudal peduncle length	16.3	11.1–16.3	14.2	1.6
Caudal peduncle depth	8.4	6.4–8.4	7.4	0.5
Predorsal length	66.2	66.1–69.9	67.5	1.0
Preanal length	65.2	62.1–65.8	64.1	1.1
Dorsal-fin base length	7.8	7.4–10.1	8.7	0.8
Anal-fin base length	25.1	20.6–26.6	23.3	1.4
Distance between dorsal-fin origin and middle of caudal-fin base	34.9	33.2–35.4	34.5	0.6
Distance between anal-fin origin and middle caudal-fin base	35.3	35.3–38.1	36.8	0.9
Pectoral girdle width	13.4	10.6–15.2	12.3	1.0
Pectoral fin length	12.9	9.2–12.9	10.9	1.2
Prepelvic length	46.6	44.1–50.9	46.8	1.7
Head length	17.1	14.8–20.9	16.7	1.3
Percentage of head length				
Head width	81.1	78.0–88.8	82.8	2.9
Head depth	43.8	37.9–53.1	47.9	3.6
Dorsal interorbital distance	53.5	47.0–57.0	52.9	2.3
Ventral interorbital distance	49.7	42.1–52.1	47.6	2.6
Snout length	45.3	45.3–53.5	48.7	2.2
Maxillary-barbel length	56.0	22.8–59.2	34.4	11.2
Rictal-barbel length	29.6	17.7–32.9	23.7	5.5
Mouth width	49.1	47.7–61.8	54.8	3.5
Eye diameter	28.7	21.2–28.7	25.2	1.7

Maxillary, rictal, and nasal barbels with thick bases, tapering distally. Maxillary barbel long, depressed, its tip reaching pectoral-fin base. Rictal barbel ventral to maxillary, its tip reaching slightly beyond posterior orbital margin. Nasal barbels absent externally, or very short in large individuals (Fig. 1). When present, continuous with lateral part of integument around anterior nostril.

Pectoral fin i,5(15*) or i,4,i(4), with round distal margin, first ray unbranched, similar in size to subsequent rays. Pelvic fin i,3,i(19), positioned entirely anterior to vertical through origins of dorsal and anal fins, approximately at midlength of SL, pelvic-fin base vertically aligned with the 13th or 14th vertebra. Dorsal fin i,5,i(6), i,6(13*), plus one procurrent ray anteriorly, trapezoidal in lateral view, its origin on posterior third of body, slightly posterior to vertical through anal-fin origin. Anal fin i,20(2), ii,20(2), i,21(10*), i,22(3) or i,23(2), plus one procurrent ray anteriorly, elongate, triangular in profile with straight distal margin, rays decreasing in size posteriorly. Caudal-fin 6+7(19*), bilobed with round corners, posterior margin of each lobe gently convex. Procurrent caudal-fin rays 8(1), 9(2), 10(5), or 12(1) ventrally, 8(2), 9(6), or 10(1) dorsally.

Internal morphology. Neurocranium roof mostly absent, with single wide skull fontanelle (Fig. 2). Anterior margin of mesethmoid approximately straight to slightly concave in medial portion. Mesethmoid cornua elongate, slender posteriorly, reaching approximately two-thirds maxilla length, distal margins slightly curved anteriorly. Mesethmoid axis extremely thin, covered posterodorsally by frontal. Frontal elongated, thin posteriorly, wider anteriorly, no contact in sagittal portion. Sphenotic, prootic, and pterosphenoid fused, anterolaterally articulated with hyomandibular. Pterotic with relatively long lateral process, approximately half length of posttemporo-supracleithrum. Lateral ethmoid small, narrow, connected to orbitosphenoid by cartilage. Orbitosphenoid slightly trapezoidal, with large foramen ovale bordered by thin laterodorsal bony lamina. Presence of laterodorsal process on orbitosphenoid, connected by cartilage/tendon to pterosphenoid end.

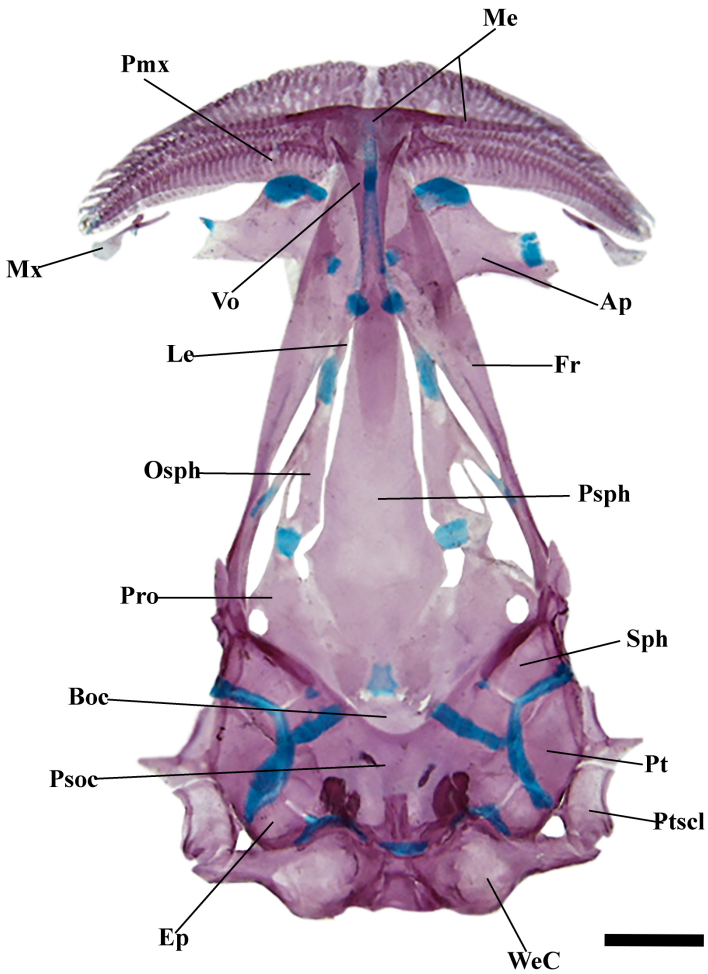

FIGURE 2 | Neurocranium of *Tridensimilis magnus*, UFOPA 1773, 28.5 mm SL; dorsal view. Ap, autopalatine; Boc, basioccipital; Ep, epioccipital; Fr, frontal; Le, lateral ethmoid; Me, mesethmoid; Mx, maxilla; Osph, orbitosphenoid; Psph, parasphenoid; Psoc, parieto-supraoccipital; Ptscl, postemporosupracleithrum; Pmx, premaxilla; Pro, sphenotic-prootic-pterosphenoid; Pt, pterotic; Sph, sphenotic-prootic-pterosphenoid; Vo, vomer; WeC, Weberian capsule. Scale bar = 0.3 mm.

Premaxilla large in proximal region, tapering distally (sickle-shaped), slightly concave towards mouth rictus, with presence of anteromedial ascending process articulated with mesethmoid cornua. Premaxilla with three rows of curved teeth (hook-shaped), two rows of teeth embedded in fleshy upper lips; premaxilla articulates with anteromedial edge of palatine. Maxilla short, narrow anteriorly, paralleling posterior third of premaxilla; short midlateral process, posteriorly expanded to tip; supporting distally base of maxillary and rictal barbels. Lower jaw triangular; Meckel's cartilage located ventrally in distal third of lower jaw. Coronomeckelian bone absent. Dentary with numerous conical, curved teeth arranged in five rows, including two or three anteromedial symphyseal teeth.

Autopalatine with broad anterior cartilage and two processes: one lateral, slightly wider with cartilage near tip, articulating with the dentary; one thin, long ventral process. Quadrate long, slender, about same length as longitudinal axis of hyomandibula, with short and narrow anterodorsal process. Metapterygoid absent. Hyomandibula with wide distal process, oriented anterodorsally. Interopercle articulated lateroventrally with preopercle, dorsally with opercle, axes approximately same size (Fig. 3).

Parurohyal with conspicuous hypobranchial foramen, elongated; long, thin lateral process nearly reaching first branchial ray; short, laminar posterior process. Hyoid arch with ventral hypohyal trapezoidal. Anterior ceratohyal elongated, slightly narrower medially. Posterior ceratohyal short, slightly rectangular, distally rounded. Six branchiostegal rays: 1st–3rd articulating with anterior ceratohyal, 4th–6th with posterior ceratohyal; 5th and 6th notably distally expanded (Fig. 4). Gill arches with basibranchials and hypobranchials completely cartilaginous. Basibranchials 2 and 3 fused, elongated; basibranchial 4 large, quadrate in shape. Hypobranchial 1 narrow, elongated; hypobranchial 2 with anterior process, narrow, shorter than 1 and 3; hypobranchials

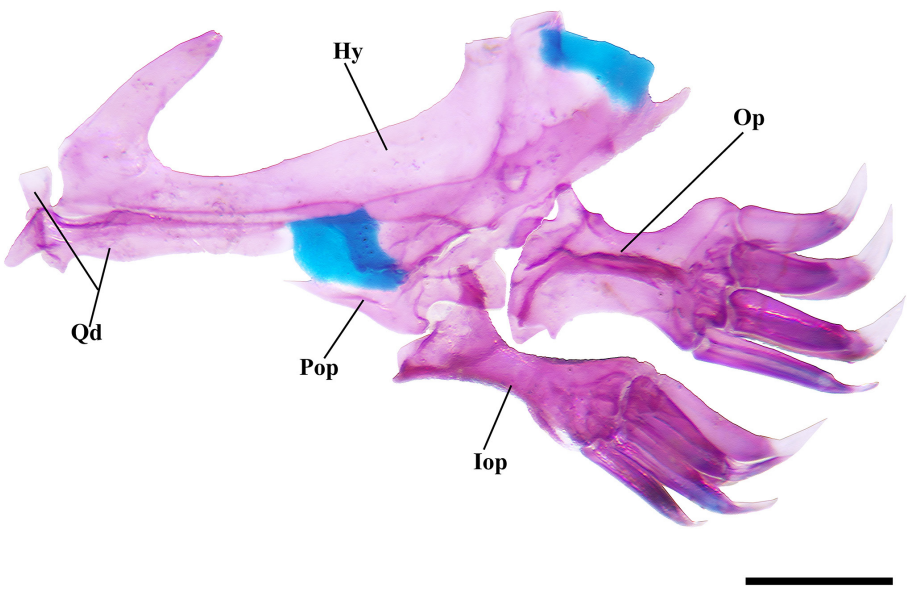

FIGURE 3 | Suspensorium and opercular series of *Tridensimilis magnus*, left lateral view, paratype, UFOPA 1773, 28.5 mm SL; Hy, hyomandibular; Iop, interopercle; Op, opercle; Pop, preopercle; Qd, quadrate. Scale bar = 0.2 mm.

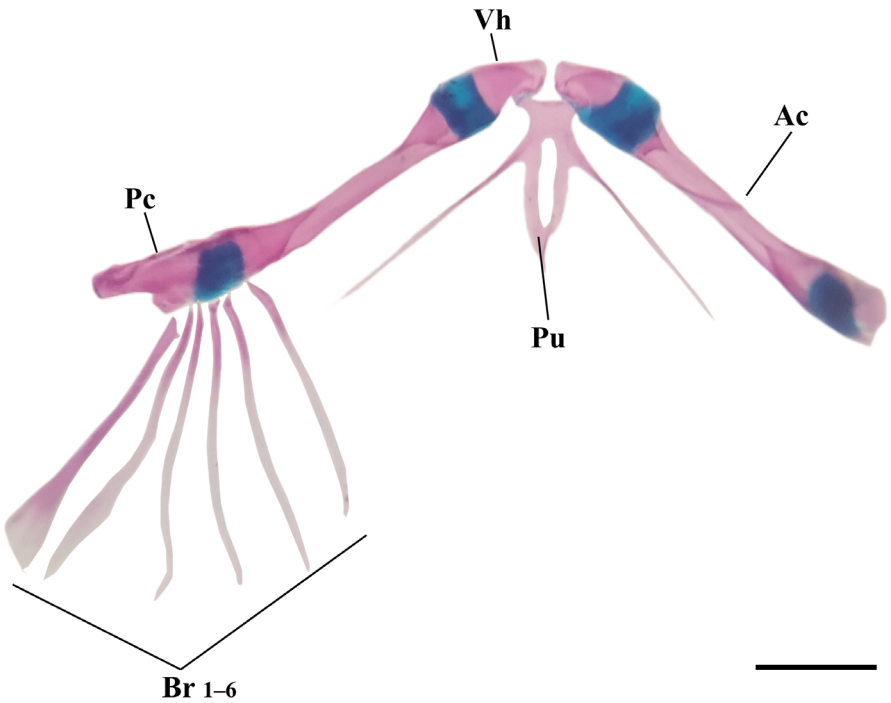

FIGURE 4 | Hyoid arch of *Tridensimilis magnus*, ventral view, paratype, UFOPA 1773, 28.5 mm SL. Ac, anterior ceratohyal; Br (1–6), branchiostegal rays; Pc, posterior ceratohyal; Pu, parurohyal; Vh, ventral hypohyal. Scale bar = 0.2 mm.

3 broad, slightly rectangular, with medial concavity. Ceratobranchials long, slender, ossified mid-portion, cartilaginous at ends; ceratobranchial 5 with two to four short teeth. Epibranchials 1–3 cartilaginous, narrow, elongated; epibranchial 4 robust, mostly cartilaginous, slightly ossified. Pharyngobranchial 4 cartilaginous, long, and rod-like, associated with upper pharyngeal tooth plate. Pharyngeal tooth plate arched, with eight or nine conical teeth of varying sizes (Fig. 5).

Weberian apparatus encapsulated, with neck-like lateral constriction, small lateral opening; distal margin articulates with basioccipital (Fig. 2). Post-Weberian vertebrae 39(2), 40(6), or 41(1). Three pairs of pleural ribs. The first post-Weberian vertebra is slightly smaller than subsequent ones. First hemal arch complete from 6th post-Weberian vertebra. Posttemporo-supracleithrum articulated to neurocranium. Cleithrum with marginal ossification. Scapulo-coracoid fully cartilaginous below 28 mm SL; partially cartilaginous in larger individuals. Three pectoral radials entirely cartilaginous in specimens below 28 mm SL; partially cartilaginous in larger individuals. Pelvic girdle elements exhibit ontogenetic variation, as observed in elements of pectoral girdle (Fig. 6). Smaller specimens possess all cartilaginous elements, with basipterygia fused sagittally; larger specimens exhibit ossifications on anterolateral and anteromedial spines. Dorsal-fin basal radials 7(7) or 8(2); first inserted anterior to neural spine of 21st (1), 22nd (5), or 23rd (3) post-Weberian vertebrae. Anal-fin basal radials 21(4), 22(1), or 23(4); first inserted anterior to haemal spine of 20th (2), or 21st (7) post-Weberian vertebrae (Fig. 7). Caudal skeleton with compound centrum (PU1+U1); neural arch

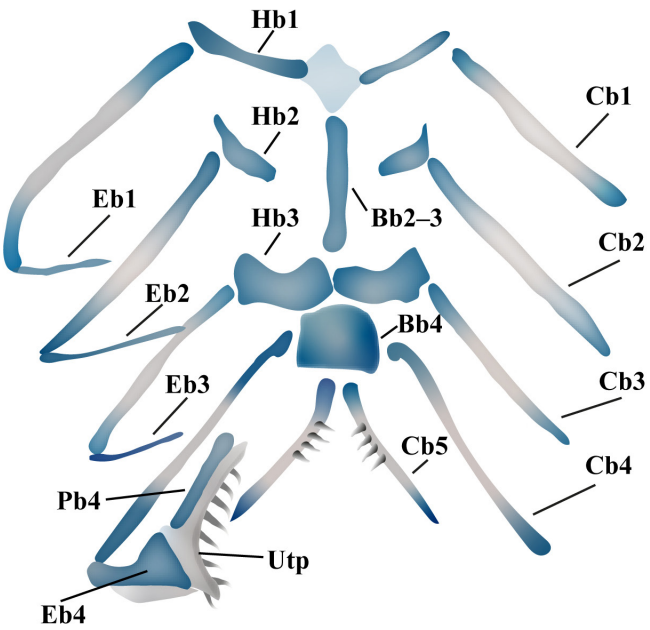

FIGURE 5 | Gill arches of *Tridensimilis magnus*, digital illustration of c&s specimen, dorsal view, paratype, UFOPA 1773, 28.5 mm SL; right dorsal elements not shown. Bb1-4, basibranchials 1 to 4; Cb1-5, ceratobranchials 1 to 5; Eb1-4, epibranchials 1 to 4; Hb1-3, hypobranchials 1 to 3; Pb4, pharyngobranchial; Utp, upper pharyngeal tooth plate. Scale bar = 0.1 mm.

incomplete; parhypural and hypurals 1 and 2 fused, forming trapezoidal lower hypural plate; upper hypural plate with two elements, hypural 3 autogenous, hypurals 4 and 5 fused; pleurostyle present, anterodorsal to hypural 5 plate; epural absent (Fig. 8).

Laterosensory system. Head sensory canals are non-dendritic, continuous, and interconnected tubes ending in single pores. Nasal and frontal canals of supraorbital line continuous, with three bilateral pores: s1 dorsal to midlength of mesethmoid cornua, posteromedial to anterior nostril; s3 above and between anterior frontal portion and mediolateral to autopalatine, just posterior to posterior nostril; s6 lateral to distal tip of hyomandibular process, between eyes on medial portion. Infraorbital canal reduced to short branch ending in pore i11, connected to neurocranium via opening between frontal and anterior portion of sphenotic-prootic-pterosphenoid, dorsolateral to orbit. Postoptic (temporal) canal with two branches and pores: po1 connected to neurocranium between posterolateral and anterolateral borders of sphenotic and pterotic, dorsoanterior to opercular odontodophore; po2 near tip of posterolateral process of pterotic, dorsolaterally to opercular odontodophore. Lateral-line canal short, with two pores (ll1, ll2), extending from posterodorsal extremity of posttemporo-supracleithrum, posterior to opercular odontophore, to vertical through middle of pectoral fin.

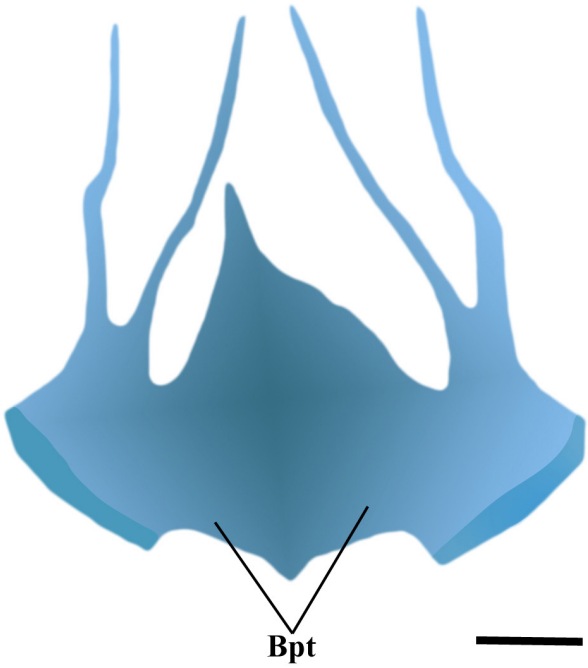

FIGURE 6 | Pelvic girdle of *Tridensimilis magnus*, digital illustration of c&s specimen, ventral view, paratype, UFOPA 1773, 28.5 mm SL. Bpt, basipterygium. Scale bar = 0.1 mm.

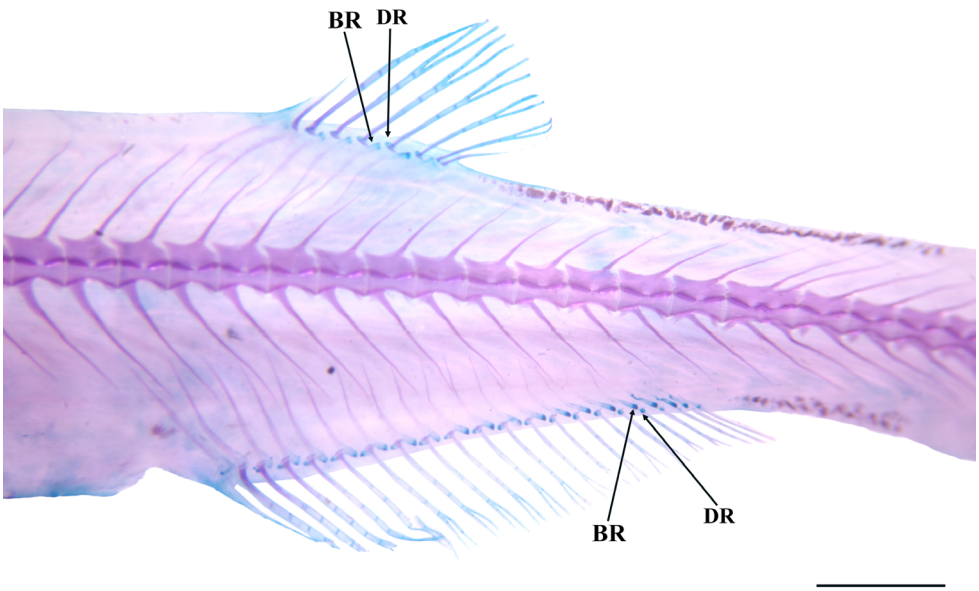

FIGURE 7 | Anal and dorsal fins of *Tridensimilis magnus*, paratype, left lateral view, UFOPA 1773, 28.5 mm SL. Arrows indicate the basal (BR) and distal (DR) radials of the fins. Scale bar = 0.1 mm.

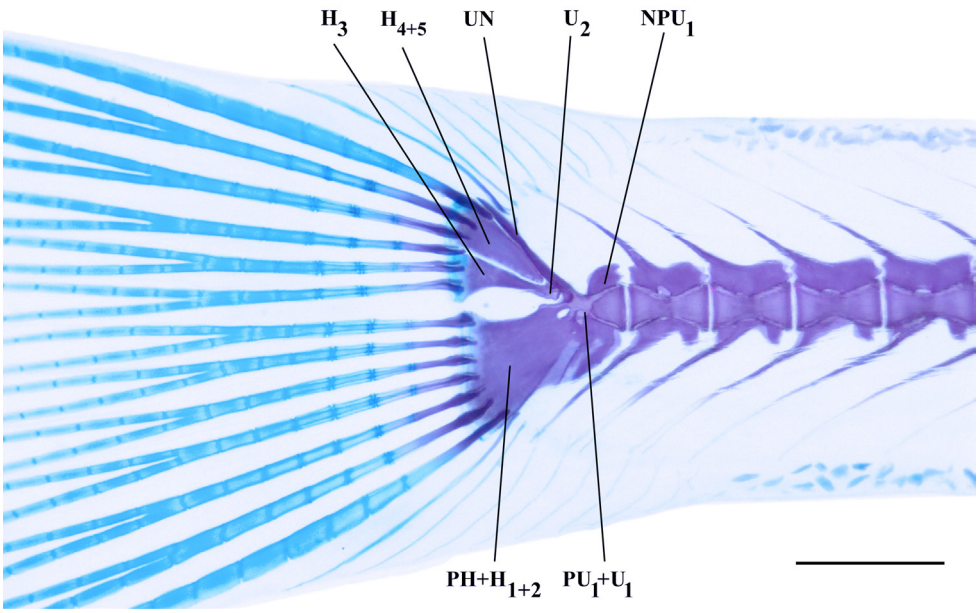

FIGURE 8 | Caudal skeleton of *Tridensimilis magnus*, paratype, left lateral view, UFOPA 1773, 28.5 mm SL. PU_1+U_1, compound centrum; NPU_1, neural preural 1; U_2, ural centrum 2; UN, uroneural; $PH+H_{1+2}$ parhypural and hypurals 1 and 2; H_3, hypural 3; H_{4+5}, hypurals 4, and 5. Scale bar = 0.2 mm.

Coloration in alcohol. Overall coloration of head and body uniformly white to pale yellow (Fig. 1). Strikingly dark patch at middle of head between eyes and posteriorly to head attachment, formed by large brain melanophores roughly outlining central part of neurocranium, more concentrated posteriorly. Two broad dark semicircles anteromedian to eyes, formed by internal dark chromatophores surrounding olfactory rosettes. Semicircles less clearly visible externally than brain pigment due to thicker cover of soft tissues. Few dispersed melanophores on opercular and interopercular odontodophores, concentrated centrally and around internal rim of periodontodal fold on each structure. Maxillary, rictal, and nasal barbels white. Dorsum with covering of dark chromatophores, sparse anteriorly and progressively more concentrated medially towards dorsal fin. Dorsal surface of caudal peduncle with well-defined dark band formed by dense covering of dark chromatophores. Lateral surface of trunk with faint row of single dark chromatophores along lateral midline (coinciding with longitudinal skeletogenous septum) from vertical through distal margin of pectoral fin to end of caudal peduncle. Posterior third of caudal peduncle also with internal dark chromatophores around vertebral centra visible by transparency, posteriorly extending in narrow oblique line along urostyle. Abdomen with cloud of peritoneal melanophores along dorsal margin of abdominal cavity, visible laterally as dark cloud from region posterior to pectoral fin to anus. Row of melanophores along ventral midline, from midpoint between pectoral fin to anterior end of pelvic girdle, reappearing posteriorly from region between pelvic fins to origin of anal fin. Ventral margin of caudal peduncle with irregular concentration of dark chromatophores. All fins with rows of melanophores along margin of rays, more concentrated basally. Pectoral fin with curved dark line at base, following margin of muscular base. Pelvic fin with well-defined straight thin dark

line across base. Base of dorsal fin with row of dark chromatophores forming oblique line. Base of anal fin with two dark lines, mostly parallel in paths but diverging in intensities: dorsal one along limit between hypaxial musculature and anal-fin muscles, denser anteriorly, and ventral one formed by single file of chromatophores positioned on base of each ray, denser posteriorly. Caudal fin with small dark concentrations on corners of hypural plate, extending dorsally and ventrally along limits of upper and lower principal rays. Middle of caudal fin hyaline. Axillary gland yellowish, contrasting with mostly white remainder of body surface.

Coloration in life. Entire body highly transparent, with most internal structures (vertebral centra, hemal and neural spines, pterygiophores, caudal skeleton) readily visible. Ventral margin of vertebral column darker than remaining tissues, corresponding to dorsal aorta. Gut and abdominal organs also visible, with swallowed air bubbles in stomach and intestines clearly evident. Refractivelly-differentiated large globular corpuscles congregated along nearly entire dorsal margin and posterior two-thirds of ventral margin of caudal peduncle, possibly representing adipose bodies. Head whitish, not as transparent as body, with branchial region pinkish due to blood visible through transparency. Eye black centrally and iridescent silver peripherally. Dark pigmentation of body similar to those of preserved specimens, but barely evident in photographs available of live specimens, perhaps because of dark background used (Fig. 9).

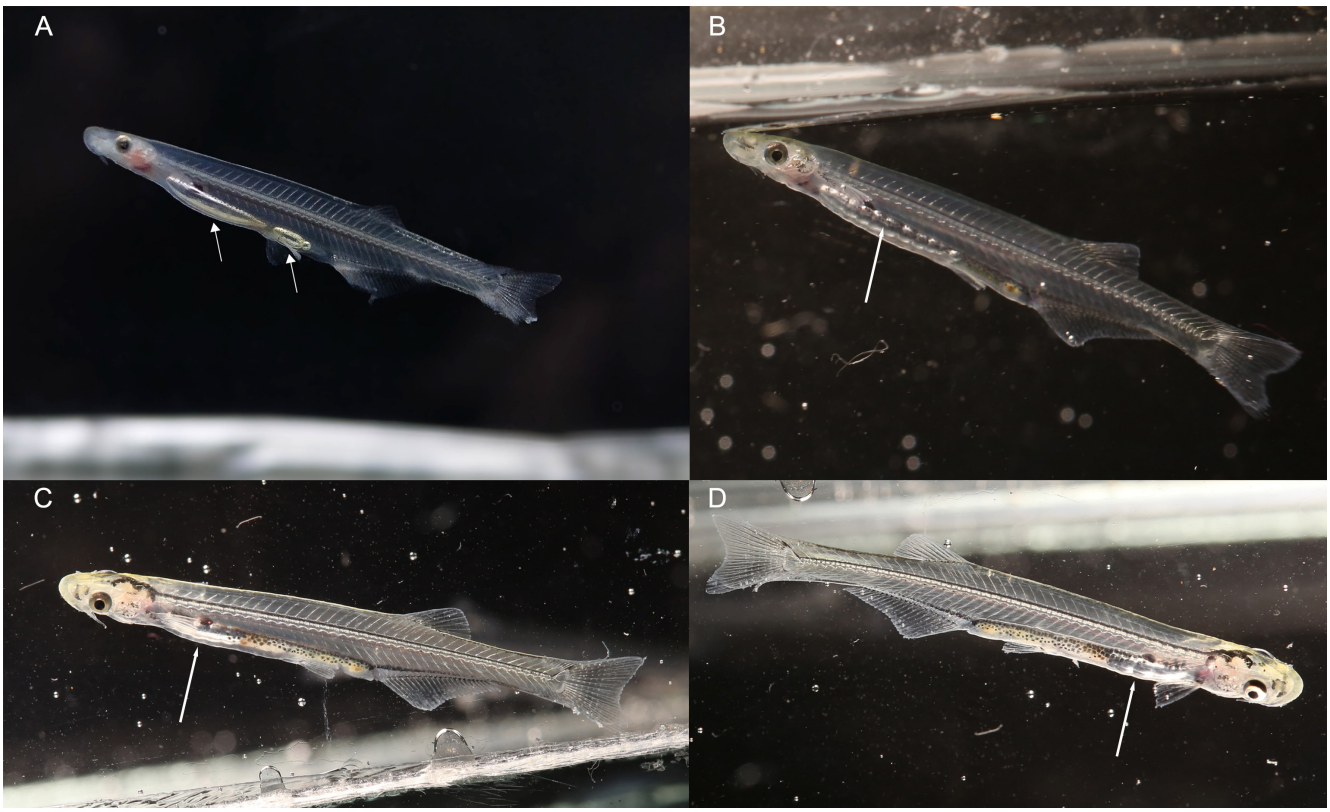

FIGURE 9 | Live specimens of *Tridensimilis magnus*: UFOPA-I 1773, 29.0 mm SL (A) and INPA-ICT 62042, not mensured (B-D). Arrows indicate swallowed air bubbles in stomach and intestines.

Geographical distribution. *Tridensimilis magnus* is known from the upper and middle rio Tapajós basin, including rios Teles Pires, Jamanxim, das Tropas, and Pacu, and small left-bank tributaries (igarapés da Montanha, Limão, and Miaçu) (Fig. 10).

Ecological notes. The rio Aruri Grande, type locality of *Tridensimilis magnus* (Fig. 11), has clear waters. At time of collecting, physicochemical parameters were temperature 24.9°C, pH 5.9, conductivity 27.4 µS/cm^3, and dissolved oxygen 5.88 mg/L. At the collecting site, the river is approximately 9 m wide and 50 cm deep, with slow flow. The locality has extensive riparian forest cover. *Tridensimilis magnus* specimens were captured exclusively in the dry season, primarily on sandbanks or small beaches along margins. Substrate predominantly consisted of coarse yellow sand. The species shares its habitat with three other trichomycterids: *Ochmacanthus reinhardtii* (Steindachner, 1882), *Stegophilus panzeri* (Ahl, 1931), and *Hyaloglanis nheengatu* (Canto, Hercos & Ribeiro, 2022).

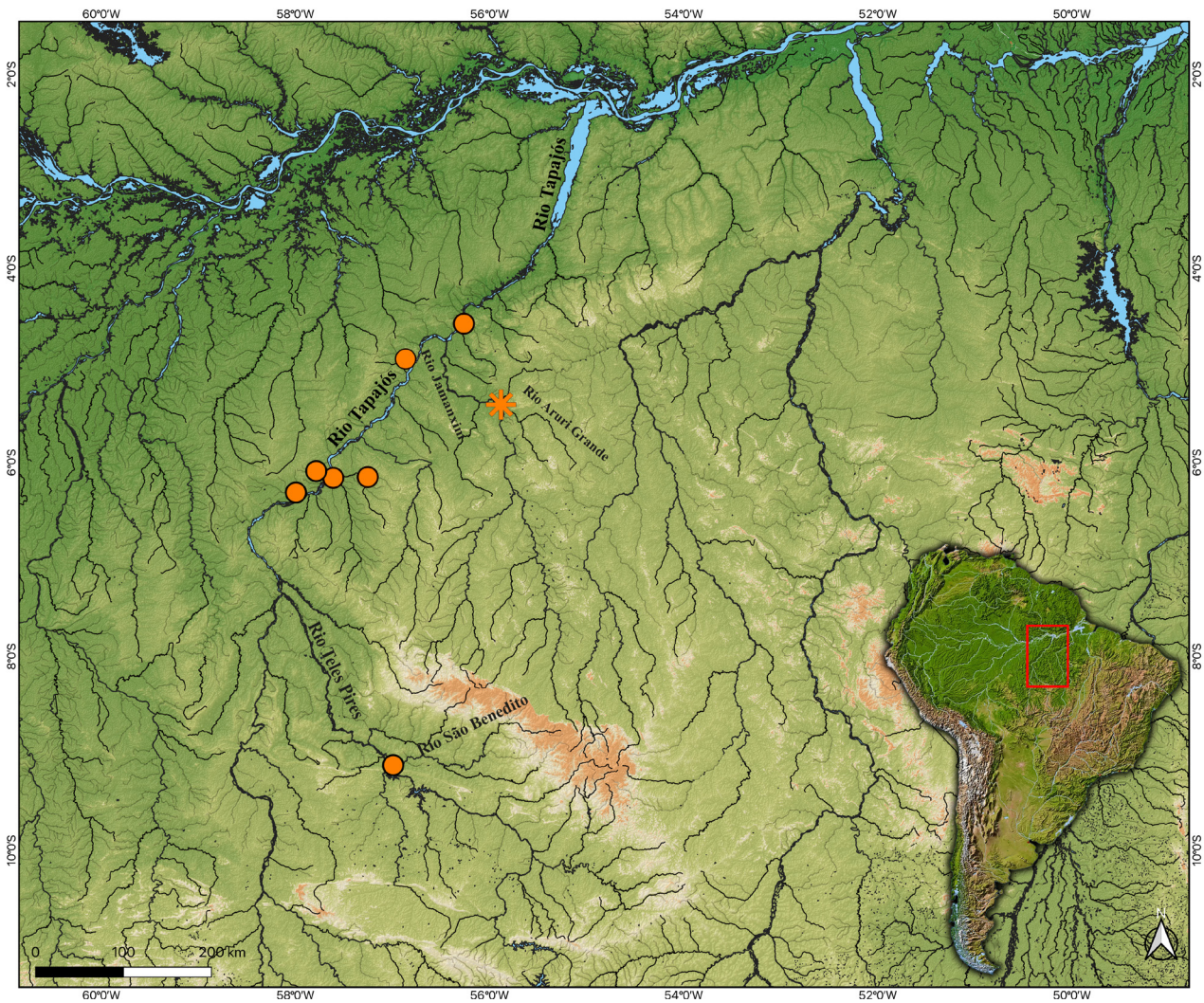

FIGURE 10 | Geographic distribution of *Tridensimilis magnus*. Orange asterisk indicates the type locality; orange circles represent paratypes.

FIGURE 11 | Type locality of *Tridensimilis magnus*, igarapé Branco, tributary to rio Aruri Grande, rio Jamanxim drainage, rio Tapajós drainage, Pará State, Brazil.

Conservation status. *Tridensimilis magnus* is known from several localities along the rios Tapajós and Teles Pires drainages, from the main river channel to smaller tributaries. Those regions have faced significant impacts due to population growth, which has heightened anthropogenic pressures, including illegal logging, expansion of agricultural frontiers, and gold mining activities (Fearnside, 2015; Lobo *et al*., 2015). The southwest of the state of Pará is a region notorious for extensive anthropogenic impact. Despite that, the smaller tributaries where the species has been recorded drain relatively well-preserved areas surrounded by legally protected areas, such as the Amazon National Park and the Jamanxim National Park (Canto *et al*., 2022).

The new species exhibits a wide Extent of Occurrence and appears to be abundant at collection sites. Furthermore, no continuous decline has been observed in population, area of occupancy or number of locations or subpopulations. Therefore, according to the categories and criteria established by the International Union for Conservation of Nature (IUCN Standards and Petitions Committee, 2024), we suggest that *T. magnus* be classified as Least Concern (LC).

Etymology. The specific epithet *magnus* derives from Latin meaning "large" or "great", in allusion to the longer length of the species in comparison to its congeners, emphasizing one of the distinctive morphological traits that diagnose the species. An adjective.

Remarks on the behavior of *Tridensimilis magnus*. Specimens of *T. magnus* were transported alive to laboratory for capturing images of live individuals. Some observations on behaviour were made during that process. Most conspicuously, specimens exhibited a behavior of capturing atmospheric air at the water surface, visibly filling the digestive cavity with air bubbles (see Fig. 9). Apparently, this behavior is not exclusive. The presence of air bubbles in the digestive cavity is also observed in the photograph of the live specimen of *T. chicomendesi* by Henschel *et al*. (2023; fig. 14). Accessory aerial respiration via the gut has been reported for many Loricarioidei and may be general for the group (Podkowa, Goniakowska-Witalinska, 2003; Da Cruz *et al*., 2013). The air thus internalized necessarily has some degree of physical effect on buoyancy on all taxa. Whether this represents a motile adaptation, exclusive or additional to respiration, remains to be investigated. A buoyancy function possibility is particularly enticing in tridentines, given that at least some members of the subfamily are midwater swimmers for at least part of their time.

At all collecting sites, *T. magnus* was found in habitats with predominantly sandy substrates. At the type locality and in the igarapé Miaçú, specimens were collected during the day. In contrast, specimens collected at other sites along the rio Tapajós were captured at dusk or in the early night, swimming in the mid-water column. These observations indicate a flexible pattern of habitat use. Individuals remain associated with sandy substrates, resting on or partially buried in the sand during daylight hours for concealment, and ascend to the water column at twilight, presumably to forage. This pattern is consistent with the adaptations reported for some psammophilous fish species (*e.g*., *Gymnorhamphichthys rondoni* (Miranda Ribeiro, 1920), *Mastiglanis asopos* Bockmann, 1994, and *Pygidianops amphioxus* de Pinna & Kirovsky, 2011), which often remain partially buried in or resting on the sandy bottom during the day, exhibiting cryptic coloration to blend with the substrate, as well as reduced daytime activity and nocturnal foraging (Zuanon *et al*., 2006; Carvalho *et al*., 2014).

DISCUSSION

The subfamily Tridentinae remains one of the least studied groups within Trichomycteridae, with significant gaps in taxonomic, phylogenetic, and ecological knowledge (de Pinna *et al*., 2024). Despite recent taxonomic advancements, such as the description of new species and the establishment of a new genus, the phylogenetic relationships among some of its members remain unresolved, especially the delimitation of certain genera. Nevertheless, the monophyly of Tridentinae is well-supported by morphological and molecular evidence (Baskin, 1973; de Pinna, 1998; Ochoa *et al*., 2017, 2020). Historically, the subfamily Tridentinae has been poorly studied due to the scarcity of specimens in scientific collections, their small body size, and the apparent morphological similarities among its members. Current knowledge of Tridentinae diversity, particularly in the Amazon basin, remains limited, partly because of well-known challenges such as sampling difficulties and frequent misidentifications.

The systematics of the genera within Tridentinae was recently revised by Datovo *et al.* (2023). Within that framework, *Tridensimilis magnus* is unequivocally placed in Tridentinae, as it exhibits all features regarded as synapomorphies of the subfamily:

[1] cranial roof largely unossified, forming a single greatly enlarged fontanel (Fig. 2; *vs*. ossified roof with none, one, or two small fontanels); [2] maxilla extremely reduced, proportionally the smallest in the family (Fig. 2; *vs*. larger maxilla); [3] eyes exposed ventrally (Fig. 1; *vs*. not ventrally exposed); [4] opercular and interopercular odontodophores juxtaposed, separated by a gap smaller than the depth of the opercular patch (Fig. 3; *vs*. gap greater than patch depth); [5] opercle with an anteroventral process shorter than the depth of its articular condyle with the hyomandibula (Fig. 3; *vs*. process longer than condyle depth); [6] dorsal-fin origin at the same level or posterior to the anal-fin origin in external view (Fig. 1; *vs*. dorsal-fin origin anterior to anal-fin origin); [7] anterior portion of hyomandibula bearing a distal dorsal process (Fig. 3; *vs*. process absent); and [8] anal fin with 15 or more rays (*vs*. 12 or fewer).

The new species also exhibits three of the four synapomorphies for the clade comprising all tridentines except *Miuroglanis* (Fig. 12): [9] anal fin with 17 or more rays (*vs*. 15 or fewer); [10] ventral exposure of the eye equal to or greater than its dorsal exposure (Fig. 1; *vs*. smaller); and [11] eyes distinctly larger than in *Miuroglanis* (Fig. 1). The fourth synapomorphy for this clade, [12] the anteriormost anal-fin pterygiophore inserting two or more vertebrae anteriorly to the anteriormost dorsal-fin pterygiophore (*vs*. one or fewer vertebrae posteriorly), is absent in *T. magnus* (inserting only one vertebra). This condition is most parsimoniously interpreted as a reversal, since *T. magnus* retains most of the synapomorphies defining this and other less inclusive clades (see below).

Tridensimilis magnus is placed within the clade comprising *Rhinotridens*, *Tridensimilis*, and *Tridens*, as it exhibits one synapomorphy defining that lineage: [13] basipterygium mostly or entirely cartilaginous in adults (Fig. 5; *vs*. largely ossified in both juveniles and adults; character inapplicable in *Miuroglanis* and *Tridens vitreus*, which lack pelvic fins and girdle; Baskin, 1973; Henschel *et al*., 2023). The second synapomorphy for that

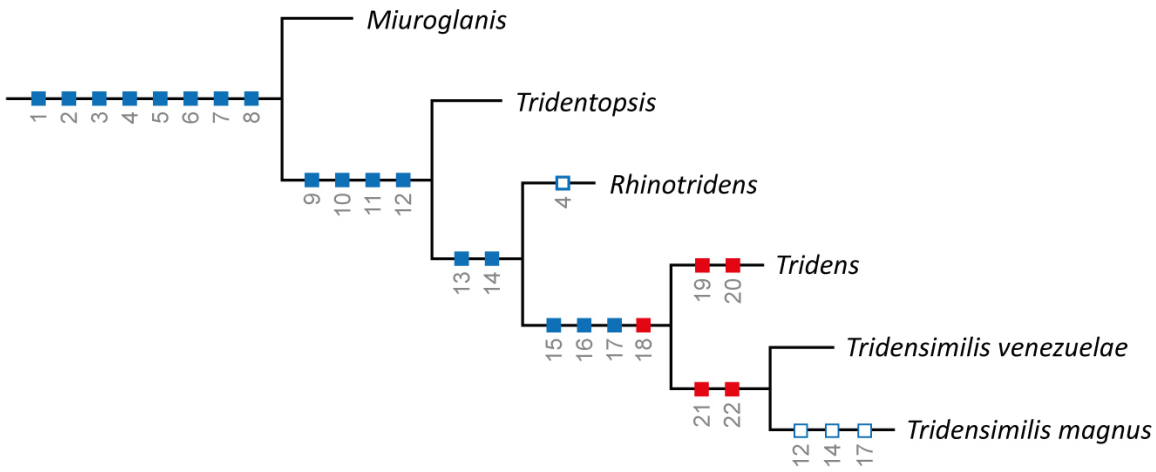

FIGURE 12 | Phylogenetic relationships of Tridentinae. Blue squares indicate characters proposed by Baskin (1973) and Datovo *et al.* (2023), and red squares indicate characters proposed in the present study. See Discussion for character numbering and explanations.

clade, [14] three to six opercular odontodes (Fig. 3; *vs*. 10–15) is not fully consistent with the condition in *T. magnus* (6–7). The validity of this character should therefore be reassessed, preferably by incorporating it into phylogenetic matrices as a quantitative trait. This pattern is not unexpected in Trichomycteridae, as variation in odontode counts tends to increase as new species are discovered.

The new species also exhibits two of the three previously recognized synapomorphies for the clade *Tridensimilis* + *Tridens*: [15] eyes facing more ventrally than dorsally (Fig. 1; *vs*. equal or more dorsally); and [16] Weberian capsule with an elongate, neck-like lateral constriction (Fig. 2; *vs*. constriction absent). As noted above, *T. magnus* has the anteriormost anal-fin pterygiophore inserting only one vertebra anterior to the anteriormost dorsal-fin pterygiophore. It therefore lacks the third synapomorphy of *Tridensimilis* + *Tridens*, namely [17] an anal-fin origin three or more vertebrae anterior to the dorsal-fin origin. On the other hand, we identified an additional apomorphic condition shared by *Tridensimilis magnus*, *T. venezuelae*, and all species of *Tridens*: [18] orbitosphenoid completely surrounding the foramen for the optic nerve (*vs.* orbitosphenoid surrounding the foramen only ventrally, in *Rhinotridens*, or anteroventrally, in the remaining tridentines). Therefore, the most parsimonious hypothesis is that the new species belongs to the clade *Tridensimilis* + *Tridens*.

The boundaries between *Tridensimilis* and *Tridens* have remained poorly defined, and neither genus has until now been supported by unequivocal phylogenetic diagnoses. To help clarify their limits and provide more robust morphological diagnoses, we propose herein new putative synapomorphies for each genus. All known species of *Tridens* [19] lack an ossified lateral ethmoid and mesethmoid axis (*vs.* ossified). Instead, the ethmoid cartilage in *Tridens* has an inverted Y-shape, with its anterior and posterior tips directly articulating with the mesethmoid cornua and the orbitosphenoid, respectively (Henschel *et al*., 2023: fig. 3). This condition is interpreted as synapomorphic for the genus, as other tridentines exhibit an ossified lateral ethmoid and at least part of the mesethmoid axis. *Tridensimilis magnus* retains the plesiomorphic condition (Fig. 2). In addition, current data indicate that *Tridens* is the tridentine genus with: [20] highest vertebral number (45–52 vertebrae *vs.* 40 or fewer).

Tridensimilis venezuelae and *T. magnus* share two osteological conditions: [21] upper hypural plate subdivided into two separate elements, presumably hypural 4+5 and hypural 3 (Fig. 8; *vs.* upper hypural plate fused into a single element, presumably hypural 3+4+5); and [22] autogenous cartilaginous distal radials present in the dorsal and anal fins (Fig. 7; *vs*. distal radials absent). Although both conditions are found elsewhere in Trichomycteridae, they are unique among tridentines. Given the current understanding of tridentine relationships (Datovo *et al*., 2023; de Pinna *et al*., 2024), the subdivided upper hypural plate and autogenous distal radials are most parsimoniously interpreted as synapomorphies of *Tridensimilis*.

Remarks on tridentine taxonomy. The reallocation of *Tridentopsis brevis* (Datovo *et al*., 2023) reveal that three of the four species currently assigned to *Tridentopsis* (*T. brevis*, *T. cahuali* Azpelicueta, 1990, and *T. pearsoni* Myers, 1925) share an externally conspicuous nasal barbel associated with the anterior nostril, measuring approximately twice the height of the surrounding skin fold. This barbel is absent or extremely reduced in *Tridentopsis tocantinsi* and all other known tridentines, as well as in stegophilines and

vandelliines (DoNascimiento, 2013; Datovo *et al*., 2023). This evidence together with the current understanding of *Tridensimilis* and tridentine phylogeny leads us to question the current generic placement of *Tridentopsis tocantinsi*. This species is known only from its type series, and its allocation to that genus was proposed at a time when only two genera (*Tridentopsis* and *Tridens*) and four species of Tridentinae were recognized (*vs*. five genera and 12 species at present). Radiographs of the holotype of *T. tocantinsi* suggest that the species possesses an apparently separated upper caudal plate [character 21], a condition otherwise known only in *Tridensimilis* and interpreted as a putative synapomorphy of the genus (Fig. 12). Photographs of the holotype further suggest that the eyes of *T. tocantinsi* are more exposed ventrally than dorsally, a synapomorphic condition for the *Tridensimilis* + *Tridens* clade [character 15] (Fig. 12). In addition, *T. tocantinsi* apparently lacks the nasal barbel, a condition that, within Tridentinae, is otherwise known only in *Miuroglanis*, *Rhinotridens*, *Tridens* and *Tridensimilis*. Taken together, these characters strongly suggest that *T. tocantinsi* may in fact be belong to *Tridensimilis*, but a formal generic transfer is not proposed here pending the acquisition of additional evidence and further analysis on the morphology of *T. tocantinsi* and the other species of *Tridentopsis*.

Comparative material examined. Same listed in Datovo *et al*. (2023) and de Pinna *et al.* (2024), plus **Bolivia.** Amazon basin: *Tridentopsis pearsoni*, CAS 56200, 1 c&s paratype, 20.7 mm SL; CAS 28259, 4 of 17 paratypes, 20.2–21.4 mm SL. **Brazil.** Amazon basin: *Miuroglanis platycephalus*, INPA-ICT 34647, 6 of 11, 13.7–14.9 mm SL; INPA-ICT 42080, 3, 12.9–14.1mm SL; MZUSP 106970, 4, 1 c&s, 12.6–14.8 mm SL. *Rhinotridens chromocaudatus*: INPA-ICT 33819, 25 of 61, 5 c&s, 15.2–16.9 mm SL. LBP 12070, 6, 3 c&s, 16.2–16.7 mm SL. *Rhinotridens britskii* INPA-ICT 62161, 15 of 33, 14.6–16.2 mm SL. *Tridens vitreus*, INPA-ICT 59883, 2, 1 c&s paratypes, 15.2–16.4 mm SL. *Tridens* cf. *melanops*, INPA-ICT 56579, 1, 17.1 mm SL; UFOPA-I 1775, 20, 2 c&s, 17.1–22.8 mm SL. *Tridens* sp. INPA-ICT 42138, 15 of 45, 2 c&s, 14.6–22.9 mm SL. *Tridentopsis pearsoni*, LBP 13944, 7 of 10, 24.9–21.1mm SL. Paraguay basin: *Tridentopsis cahuali*, ZUFMS-PIS 5499, 3, 19.6–21.9 mm SL; ZUFMS-PIS 8184, 9, 1 c&s, 20.2–22.2 mm SL. Tocantins basin: *Tridentopsis tocantinsi*, AMNH 13967, x-ray holotype, 23.0 mm SL. **Venezuela.** Maracaibo basin: *Tridensimilis venezuelae*, UF 30742, 3, 1 c&s, 20.1–22.5 mm SL.

ACKNOLEDGMENTS

We thank David Catania (CAS), Lúcia R. Py-Daniel (INPA), Claudio Oliveira (LBP), Carolina Doria (UNIR) and George Mattox (UFSCAR), and Francisco Severo Neto (ZUFMS), for granting access to the specimens in the collections under their care. We also thank Alexandre Hercos for the collected specimens and for the image of the type locality.

REFERENCES

- **Arratia G, Huaquin L.** Morphology of the lateral line system and of the skin of diplomystid and certain primitive loricarioid catfishes and systematic and ecological considerations. Bonn Zool Monogr. 1995; 36:1–110.
- **Baskin JN.** Structure and relationships of the Trichomycteridae. [PhD Dissertation]. New York: City University of New York; 1973.
- **Canto ALC, Hercos AP, Ribeiro FRV.** Description of a new species of miniature catfish of the genus *Ammoglanis* (Siluriformes: Trichomycteridae) from rio Tapajós basin, Brazil. Neotrop Ichthyol. 2022; 20(2):e210122. https://doi.org/10.1590/1982-0224-2021-0122
- **Carvalho MS, Zuanon J, Ferreira EJG.** Diving in the sand: the natural history of *Pygidianops amphioxus* (Siluriformes: Trichomycteridae), a miniature catfish of Central Amazonian streams in Brazil. Environ Biol Fish. 2014; 97:59–68. https://doi.org/10.1007/s10641-013-0123-9
- **da Cruz AL, Silva HR, Lundstedt LM, Schwantes AR, Moraes G, Klein W *et al*.** Air-breathing behavior and physiological responses to hypoxia and air exposure in the air-breathing loricariid fish, *Pterygoplichthys anisitsi*. Fish Physiol Biochem. 2013; 39:243–56. https://doi.org/10.1007/s10695-012-9695-0
- **Datovo A, Ochoa L, Vita L, Presti P, Ohara WM, de Pinna MCC.** A new genus and species of miniature tridentine catfish from the Amazon basin (Siluriformes: Trichomycteridae). Neotrop Ichthyol. 2023; 21(3):e230076. https://doi.org/10.1590/1982-0224-2023-0076
- **DoNascimiento CL.** Sistemática y relaciones filogenéticas de la subfamilia de bagres parásitos Stegophilinae (Siluriformes, Trichomycteridae). [PhD Dissertation]. Caracas: Facultad de Ciencias, Universidad Central de Venezuela; 2013.
- **Eigenmann CH.** The Pygidiidae, a family of South American catfishes. Mem Carnegie Mus. 1918; 7:259–398.
- **Eigenmann CH, Eigenmann RS.** Preliminary notes on South American Nematognathi. II. Proc Calif Acad Sci. 1889; 2:28–56.
- **Fearnside PM.** Amazon dams and waterways: Brazil's Tapajós Basin plans. Ambio. 2015; 44(5):426–39. https://doi.org/10.1007/s13280-015-0642-z
- **Fricke R, Eschmeyer WN.** Eschmeyer's catalog of fishes: genera, species, references [Internet]. San Francisco: California Academy of Science; 2025a. Available from: http://researcharchive.calacademy.org/research/ichthyology/catalog/fishcatmain.asp
- **Fricke R, Eschmeyer WN.** A guide to fish collections in the catalog of fishes database [Internet]. San Francisco: California Academy of Science; 2025b. Available from: http://researcharchive.calacademy.org/research/ichthyology/catalog/collections.asp
- **Henschel E, Ohara WM, Costa WJEM.** Two new miniature translucent catfish species of the rare genus *Tridens* (Siluriformes: Trichomycteridae) from the Madeira River basin, northern Brazil. J Fish Biol. 2023; 103(1):155–71. https://doi.org/10.1111/jfb.15403
- **International Union for Conservation of Nature (IUCN). Standards and petitions committee.** Guidelines for using the IUCN Red List categories and criteria. Version 16 [Internet]. Gland; 2024. Available from: http://www.iucnredlist.org/documents/RedListGuidelines.pdf
- **Lobo FL, Costa MPF, Novo EMLM.** Time-series analysis of Landsat-MSS/TM/OLI images over Amazonian waters impacted by gold mining activities. Remote Sens Environ. 2015; 157:170–84. https://doi.org/10.1016/j.rse.2014.04.030
- **Ochoa LE, Datovo A, DoNascimiento C, Roxo FF, Sabaj MH, Chang J *et al*.** Phylogenomic analysis of trichomycterid catfishes (Teleostei: Siluriformes) inferred from ultraconserved elements. Sci Rep. 2020; 10:2697. https://doi.org/10.1038/s41598-020-59519-w
- **Ochoa LE, Roxo FF, DoNascimiento C, Sabaj MH, Datovo A, Alfaro M *et al*.** Multilocus analysis of the catfish family Trichomycteridae (Teleostei: Ostariophysi: Siluriformes) supporting a monophyletic Trichomycterinae. Mol Phylogenet Evol. 2017; 115:71–81. https://doi.org/10.1016/j.ympev.2017.07.007

- **de Pinna MCC.** Phylogenetic relationships of Neotropical Siluriformes (Teleostei: Ostariophysi): historical overview and synthesis of hypotheses. In: Malabarba LR, Reis RE, Vari RP, Lucena ZMS, Lucena CAS, editors. Phylogeny and classification of Neotropical fishes. Porto Alegre: Edipucrs; 1998. p.279–330
- **de Pinna MCC, Dagosta F.** A taxonomic review of the vampire catfish genus *Paracanthopoma* Giltay, 1935 (Siluriformes, Trichomycteridae), with descriptions of nine new species and a revised diagnosis of the genus. Pap Avulsos Zool. 2022; 62:e202262072. http://doi.org/10.11606/1807-0205/2022.62.072
- **de Pinna MCC, Reis V, Pastana MN, Datovo A.** A new species of the tridentine *Rhinotridens* from the Amazon basin (Siluriformes: Trichomycteridae). Neotrop Ichthyol. 2024; 22(2):e240025. https://doi.org/10.1590/1982-0224-2024-0025
- **Podkowa D, Goniakowska-Witalińska L.** Morphology of the air-breathing stomach of the catfish *Hypostomus plecostomus*. J Morphol. 2003; 257(2):147–63. https://doi.org/10.1002/jmor.10102
- **Schultz LP.** The catfishes of Venezuela, with description of thirty-eight new forms. Proc U S Natl Mus. 1944; 94(3172):173–338. https://doi.org/10.5479/si.00963801.94-3172.173
- **Taylor WR, Van Dyke GC.** Revised procedures for staining and clearing small fishes and other vertebrates for bone and cartilage study. Cybium. 1985; 9(2):107–19.
- **Tchernavin V.** A revision of some Trichmycterinae based on material preserved in the British Museum (Natural History). Proc Zool Soc London. 1944; 114(1–2):234–75. http://doi.org/10.1111/j.1096-3642.1944.tb00219.x
- **Zuanon JA, Bockmann FA, Sazima I.** A remarkable sand-dwelling fish assemblage from central Amazonia, with comments on the evolution of psammophily in South American freshwater fishes. Neotrop Ichthyol. 2006; 4(1):107–18. https://doi.org/10.1590/S1679-62252006000100012

AUTHORS' CONTRIBUTION

André L. Colares Canto: Conceptualization, Data curation, Formal analysis, Funding acquisition, Investigation, Methodology, Project administration, Resources, Software, Supervision, Validation, Visualization, Writing-original draft, Writing-review and editing.

Aléssio Datovo: Conceptualization, Data curation, Formal analysis, Funding acquisition, Investigation, Methodology, Project administration, Resources, Supervision, Validation, Visualization, Writing-original draft, Writing-review and editing.

Willian M. Ohara: Conceptualization, Data curation, Visualization, Writing-original draft, Writing-review and editing.

Mário C. C. de Pinna: Conceptualization, Data curation, Formal analysis, Funding acquisition, Investigation, Methodology, Supervision, Validation, Visualization, Writing-original draft, Writing-review and editing.

Frank Raynner V. Ribeiro: Conceptualization, Data curation, Formal analysis, Funding acquisition, Investigation, Methodology, Project administration, Resources, Supervision, Validation, Visualization, Writing-original draft, Writing-review and editing.

FUNDING INFORMATION

Funding is provided by Conselho Nacional de Desenvolvimento Científico e Tecnológico (CNPq # 310480/2022–1 to FRVR, #315634/2023–5 to MdP, #436763/2018–4 to ALCC and FRVR), Fundação Amazônia de Amparo a Estudos e Pesquisas (ICAAF 024/2014 to ALCC and FRVR), Fundação de Amparo à Pesquisa do Estado de São Paulo (FAPESP # 2023/02499–4 to AD), Instituto de Conservação Ambiental The Nature Conservancy do Brasil (Águas Tapajós Project, Cooperation BR FY20 104 and Programa de Pós-Graduação em Biodiversidade e Biotecnologia da Rede BIONORTE (PPG-BIONORTE) to ALCC and FRVR).

ETHICAL STATEMENT

The specimens, which were photographed while alive, were collected under license #65628-5, granted to WMO by the Sistema de Autorização e Informação em Biodiversidade (SISBIO). The other specimens used in this study came from zoological collections.

DATA AVAILABILITY STATEMENT

The authors confirm that the data supporting the findings of this study are available within the article.

AI STATEMENT

The authors did not use any AI-assisted technologies in the creation of this manuscript or its figures.

COMPETING INTEREST

The authors declare no competing interests.

PEER REVIEW FILE

Peer Review File

HOW TO CITE THIS ARTICLE

- **Canto ALC, Datovo A, Ohara WM, Pinna MCC, Ribeiro FRV.** A new species of *Tridensimilis* (Siluriformes: Trichomycteridae) from Tapajós basin: the largest translucent catfish species of Tridentinae. Neotrop Ichthyol. 2026; 24(2):e250209. https://doi.org/10.1590/1982-0224-2025-0209

Neotropical Ichthyology

OPEN ACCESS

SBI
Official Journal of the
Sociedade Brasileira de Ictiologia